JOURNAL OF AGRICULTURAL AND FOOD CHEMISTRY

pubs.acs.org/JAFC Article

Multiomics Analysis Revealed the Molecular Mechanism of miRNAs in Fluoride-Induced Hepatic Glucose and Lipid Metabolism Disorders

Yangfei Zhao, Yanghuan Yu, Mohammad Mehdi Ommati, Jipeng Xu, Jinming Wang, Jianhai Zhang, Zilong Sun, Ruiyan Niu, and Jundong Wang*

Cite This: *J. Agric. Food Chem.* 2022, 70, 14284−14295

Read Online

ACCESS | Metrics & More | Article Recommendations | Supporting Information

ABSTRACT: Fluoride-induced liver injury seriously endangers human and animal health and animal food safety, but the underlying mechanism remains unclear. This study aims to explore the mechanism of miRNAs in fluoride-induced hepatic glycolipid metabolism disorders. C57 male mice were used to establish the fluorosis model (22.62 mg/L F^-, 12 weeks). The results indicated that fluoride increased fluoride levels, impaired the structure and function, and disrupted the glycolipid metabolism in the liver. Furthermore, the sequencing results showed that fluoride exposure resulted in the differential expression of 35 miRNAs and 480 mRNAs, of which 23 miRNAs were related to glycolipid metabolism. miRNA−mRNA network analyses and RT-PCR revealed that miRNAs mediated fluoride-induced disturbances in the hepatic glycolipid metabolism. Its possible mechanism was to regulate the insulin pathway, PPAR pathway, and FOXO pathway, which in turn affected the bile secretion, the metabolic processes of glucose, the decomposition of lipids, and the synthesis of unsaturated fatty acids in the liver. This study provides a theoretical basis for miRNAs as diagnostic indicators and target drugs for the treatment of fluoride-induced liver injury.

KEYWORDS: *fluoride, glucose metabolism disorder, lipid metabolism disorder, liver injury, miRNA−mRNA network*

■ INTRODUCTION

With the rapid development of society, the discharge of fluoride-containing industrial waste and the use of fluoride-containing packaging materials and pesticides lead to excess severe fluoride content in plant food, animal food, and water.[1] For example, our laboratory's investigation found that the fluoride ion content in grasses was as high as 80−100 mg/kg.[2] Although fluoride is an essential trace element,[3] chronic fluoride intake can result in the damage of structure and function in various organs.[4] As the prominent place for material transformation and detoxification, the liver has been proven to be the first and foremost vulnerable organ to fluoride.[5] Fluoride accumulates in the liver after entering the body, which affects the metabolism and detoxification function of the liver, resulting in a metabolic disorder and homeostasis imbalance. Furthermore, the reduction of liver detoxification ability can result in the accumulation of harmful substances, affecting human and animal health and animal food safety.[5] The liver is an essential organ of glucose and lipid metabolism, which is closely related to liver detoxification ability. Therefore, exploring the mechanism of fluoride-induced hepatic glycolipid metabolism disorders has important practical significance for ensuring human health. Lots of literatures have reported that fluoride could cause massive infiltration of inflammatory liver cells; fatty degeneration; necrosis of hepatocytes; and swelling and dissolution of hepatocytes, mitochondria, and endoplasmic reticulum.[6,7] Nevertheless, the mechanism by which fluoride induces hepatic glucose and lipid metabolism disorders remains unclear.

Glucose and lipid metabolisms are critical biological processes that provide energy and substances for cells and organisms to maintain normal life activities.[8] As a metabolic organ, the liver is not only involved in the processes of glycogenolysis, carbohydrate synthesis, and gluconeogenesis but also in the processes of synthesis and transport of lipids.[9−11] Hence, the liver is a significant organ that regulates the balance of glycolipid metabolism. In studies of fluoride-induced liver damage, Trevizol et al. found that plasma glucose levels were decreased by 20%, and the expression levels of hepatic antioxidant and carboxylic acid metabolism-related proteins were increased after fluoride exposure;[12] Sharma et al. found that fluoride increased hepatic lipid peroxidation with a dose-dependence.[13] These studies suggested that fluoride can lead to hepatic glycolipid metabolism disturbances. However, its specific mechanism still needs further exploration.

MicroRNAs (miRNAs), about 18−25 nucleotides, are small single-stranded noncoding RNAs. It exerts biological activity through base-pairing with target genes to induce silencing complexes to degrade mRNA or prevent mRNA translation, ultimately inhibiting or reducing the expression level of proteins.[14] The widespread existence and evolutionary con-

Received: May 2, 2022
Revised: August 29, 2022
Accepted: October 3, 2022
Published: October 12, 2022

Table 1. Primer Sequences for RT-PCR

gene name	primer sequences	gene ID
miRNA-reverse	R: GCTGTCAACGATACGCTACGTAACG	
Rnu6 (U6)	F: GCTGTCAACGATACGCTACGTAACG	19862
mmu-miR-671-5p	F: AGGAAGCCCTGGAGGGGCTGGAG	MI0004133
mmu-miR-365-2-5p	F: AGGGACTTTCAGGGGCAGCTGTG	MI0001645
mmu-miR-221-5p	F: ACCTGGCATACAATGTAGATTTCTGT	MI0000709
mmu-miR-423-5p	F: TGAGGGGCAGAGAGCGAGACTTT	MI0004637
mmu-miR-362-5p	F: AATCCTTGGAACCTAGGTGTGAAT	MI0000763
mmu-miR-127-3p	F: CTGAAGCTCAGAGGGCTCTGAT	MI0000154
β-actin	F: AGGGAAATCGTGCGTGAC	NM_007393.5
	R: CATACCCAAGAAGGAAGGCT	
IRS2	F: CTGGCTGCGATGACAACTAC	NM_001081212.2
	R: CAGACAGGCATAGGCGGTAT	
MYC	F: ATGCCCCTCAACGTGAACTTC	NM_010849.4
	R: CGCAACATAGGATGGAGAGCA	
SREBF1	F: TCAAGGCAGACTCACTGCTG	NM_011480.4
	R: ATGGTCCCTCCACTCACCA	
GCK	F: AAGCACCGACTGTGACTGAG	NM_010292.5
	R: TCTGCTGAGCTGTGAGGAAC	
G6PC	F: TCGCGCTTGGATTCTACCTG	NM_008061.4
	R: CCGGTACATGCTGGAGTTGA	
FASN	F: GATGCTCTCCTGATCCCACAA	NM_007988.3
	R: AGTCTCACTGGAAGAGCTGTG	
HMGCR	F: TGCCTGGATGGGAAGGAGTA	NM_008255.2
	R: GCACCTCCACCAAGGCTTAT	
CYP7A1	F: AGTTTCGACATGCTCTCGCT	NM_007824.3
	R: GTGGTTCTTGGAGGTGCCTT	
PLIN1	F: TACCTAGCTGCTTTCTCGGTG	NM_175640.2
	R: GTGGGCTTCTTTGGTGCTGT	
ELOVL6	F: AGTTGTACTGGTGGGTGCAG	NM_130450.2
	R: TGGGTGGACATGGACAACTG	

servation of miRNA cause it to play a vital role in virus defense, hematopoietic process, organ formation, fat metabolism, cell proliferation, apoptosis, autophagy, etc.[15] Moreover, with the deepening of miRNA research in recent years, it has become a research hotspot to explore the mechanism of miRNA in disease and to use miRNA as a biomarker for disease diagnosis and a therapeutic target. Recent research studies have validated that miRNA plays a crucial regulatory role in the liver glycolipid metabolism. For example, miR-33 can regulate the biogenesis and transport of high-density lipoprotein (HDL) in the liver;[16] miR-802 maintains hepatic glucose and lipid homeostasis through the FXR-SHP nuclear receptor cascade.[17] Nonetheless, the regulatory mechanism of miRNAs in fluoride-induced hepatic glucose and lipid metabolism disorders has not been reported.

In this study, miRNA-sequencing (seq) and mRNA-seq were used to screen differentially expressed (DE)-miRNAs and DE-mRNAs in the liver after fluoride exposure. Then, bioinformatics technology was used for functional annotation and enrichment analysis. Furthermore, HE staining, liver fluoride content, and the levels of glutamic oxaloacetic transaminase (AST) and glutamic pyruvic transaminase (ALT) were used to assess the damage of liver morphology and function. As well as, Oil Red O staining; PAS staining; and levels of liver glycogen, triglyceride (TG), low-density lipoprotein (LDL), HDL, and total cholesterol (TC) were used to observe the effects of fluoride on hepatic glycolipid metabolism. Finally, the expression levels of glycolipid metabolism-related miRNAs and mRNAs were detected by RT-PCR. This study revealed the specific mechanism of miRNAs in fluoride-induced hepatic glycolipid metabolism disorders and provided valuable insights for the study of fluoride hepatotoxicity.

MATERIALS AND METHODS

Animals. Twenty-four C57 male mice (22−24 g) were bought from the China Institute of Radiation Research (Taiyuan, China). After 1-week adaptation, the mice were randomly divided into control group (0 mg/L sodium fluoride (NaF)) and NaF group (50 mg/L NaF). NaF was added into the drinking deionized water. The mice were allowed to drink and eat freely. This study's treatment concentration and time have been proven to establish a fluorosis model successfully.[6] After 12 weeks, blood was collected from the eyeballs of the mice, and they were sacrificed by cervical dislocation. Then, the serum and liver were collected, the mice were fasted before sample collection. The animal operations in the present study have been permitted by the Animal Care and Use Committee of Shanxi Agricultural University (Taigu, China). Three liver samples in each group were placed in dry ice and mailed to the sequencing company (Biomarker Technologies Co., Ltd., Beijing, China). Three liver samples were placed into 4% paraformaldehyde and 2.5% glutaraldehyde fixative solution for tissue sectioning and TEM experiments in the each group. The remaining samples were immediately placed in liquid nitrogen for subsequent experiments.

HE Staining. HE staining was used to observe the liver morphology. Three fresh liver samples in each group were fixed in 4% paraformaldehyde for 24 h. And the fixed livers were routinely dehydrated, made transparent and embedded, and cut into 5 μm sections. Then, the paraffin sections were deparaffinized to water and stained with hematoxylin and eosin. Finally, the liver sections were mounted with neutral resin after dehydration, and the liver morphology was observed with a microscope (DMI3000 M, Leica Microsystems operates, Wetzlar, Germany).

https://doi.org/10.1021/acs.jafc.2c03049
J. Agric. Food Chem. 2022, 70, 14284−14295

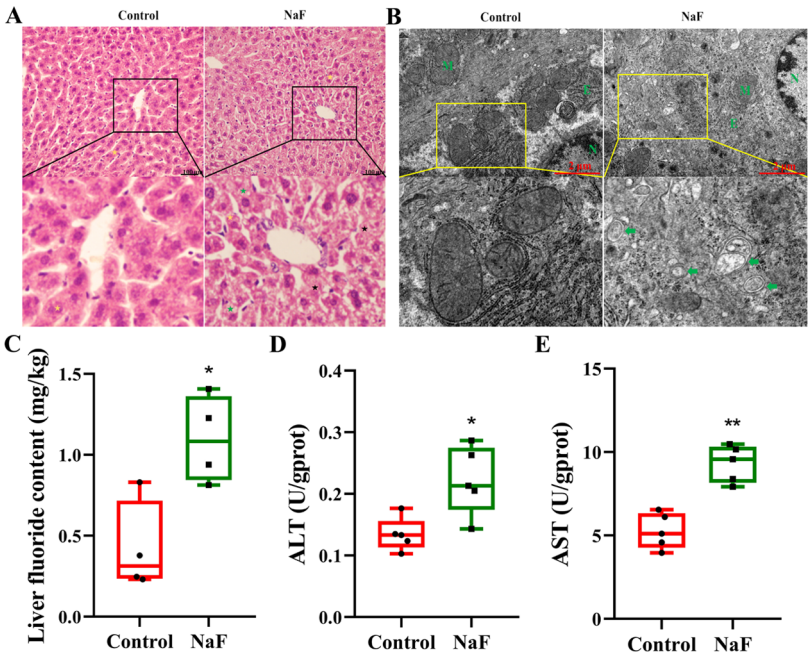

Figure 1. Effects of fluoride on the liver fluoride content, structure, and function. (A) HE staining, the yellow star: liver cord, the green star: lipid droplet, the black star: nuclear lysis; (B) TEM, E: endoplasmic reticulum, M: mitochondria, N: nucleus, green arrows: autophagosomes; (C) liver fluoride content; (D) liver ALT levels; (E) liver AST levels.

TEM. Hepatocyte ultrastructure was observed using a transparent electron microscope. In the each group, three fresh samples, approximately 1 mm^3, were fixed in 2.5% glutaraldehyde for 2 h and 1% osmium acid for 3 h. Then, the samples were dehydrated by an ethanol gradient and soaked in 100% acetone for 20 min. Finally, after embedding and solidifying, a 60 nm section was made with an ultrathin microtome (EM TXP, Leica Microsystems, Wetzlar, Germany), and the ultrastructure of hepatocytes was observed with a transmission electron microscope (HF3300, Hitachi High-Technologies Corporation, Tokyo, Japan).

Determination of Liver Fluoride Content. The liver fluoride content was detected by the fluoride ion-selective electrode method. Briefly, liver surface tissue was removed. After drying, ashing, pH adjustment, and maintaining constant volume, the liver fluoride ion contents were detected with a fluoride ion-selective electrode ($n = 5$).

Detection of Liver Function, Glucose, and Lipid Metabolism Indicators. The detections of hepatic AST and ALT contents were used to evaluate the liver function, and the detections of hepatic glycogen, LDL, HDL, TC, and TG contents were used to evaluate the hepatic glycolipid metabolism. These indicators were detected with Nanjing Jiancheng's detection kits (Nanjing, China). The experimental steps were carried out strictly following the detection kits' instructions, and the OD value was detected to analyze the results ($n = 5$).

PAS Staining. The liver glycogen was observed using the PAS staining. Paraffin sections were deparaffinized to water and incubated with periodic acid alcohol. Then, the sections were incubated with Schiff's solution and stained with hematoxylin. Lastly, the sections were routinely dehydrated to translucency and mounted with neutral resin. Under the ordinary microscope, the carbohydrates were red and the nuclei were blue. The positive area of the 400× images was counted.

Oil Red O Staining. The liver lipid was observed using the Oil Red O staining. Frozen sections (8 μm) were washed with 60% isopropanol and incubated with staining solution. After washing with 60% isopropanol, the sections were counterstained with hematoxylin. Then, the sections were mounted with glycerol gelatin after washing with water. Under the ordinary microscope, lipid droplets were orange-red and nuclei were blue. The positive area of the 400× images was counted.

miRNA-Seq and mRNA-Seq. The total mRNA extraction, library construction, library quality control, and sequencing were performed by Biomarker Technologies Co. (Beijing, China). The brief steps were as follows. After extracting the mRNA, the Nanodrop, Qubit 2.0, and Agilent 2100 bioanalyzers were used to detect the purity, concentration, and integrity of the mRNA, respectively. Then, the quality of the library was decteded by the Qubit 2.0, Agilent 2100, and Q-PCR. After quality control, the clean reads were aligned using the Bowtie software. Finally, the sequence was compared with the reference genome to get mapped reads.

DE-miRNA and DE-mRNA Screening and miRNA Target Gene Prediction. The effective sequence was aligned with the miRNA and mRNA sequence in the gene database, and the successfully aligned sequence was defined as a known miRNA and mRNA. Then, the DE-miRNAs and DE-mRNAs were screened out using the edgeR software. Finally, TargetScan 7.2 was used to predict the DE-miRNAs' target mRNAs.

Gene Ontology (GO) and KEGG Enrichment Analysis. The functions of DE-mRNAs and DE-miRNAs' target mRNAs were analyzed using the GO and KEGG enrichment analysis. Bioinformatics analysis was performed using the OmicStudio tools, Sangerbox 3.0, and Metascape.

RT-PCR Analysis. The relative expression levels of miRNAs and mRNAs were determined using RT-PCR. Total RNA and miRNA were extracted with the Trizol method and miRNA extraction kit (Shanghai Sangon Biotechnology Co., Ltd., Shanghai, China). And the NanoDrop2000 (Thermo Scientific Corporation, Massachusetts) was used to detect the quality and concentration of miRNA and mRNA. Then, the PrimeScript RT reagent Kit was used to reverse transcribe mRNA (Takara Biomedical Technology Co., Ltd., Beijing, China), and the tailed miRNA RT reagent kit was used to reverse transcribe miRNA (Shanghai Sangon Biotechnology Co., Ltd., Shanghai, China). The gene list and primer sequences were exhibited in Table 1, and U6 and β-actin were the internal reference genes. Finally, the SYBR Premix Ex Taq TM II QRT-PCR kit (Takara Biomedical Co., Ltd., Beijing, China) was used to detect the relative expressions of miRNAs and mRNAs, and the data were analyzed using $2^{-\Delta\Delta C_T}$ ($n = 6$).

Western Blotting. The protein expression levels of glycolipid metabolism key differential genes were determined using the western blotting. Briefly, total protein was extracted from 100 mg liver samples. After measuring the concentrations of the proteins with a BCA kit (Boster Biological Technology Co., Ltd., Wuhan, China), denaturation

https://doi.org/10.1021/acs.jafc.2c03049
J. Agric. Food Chem. 2022, 70, 14284−14295

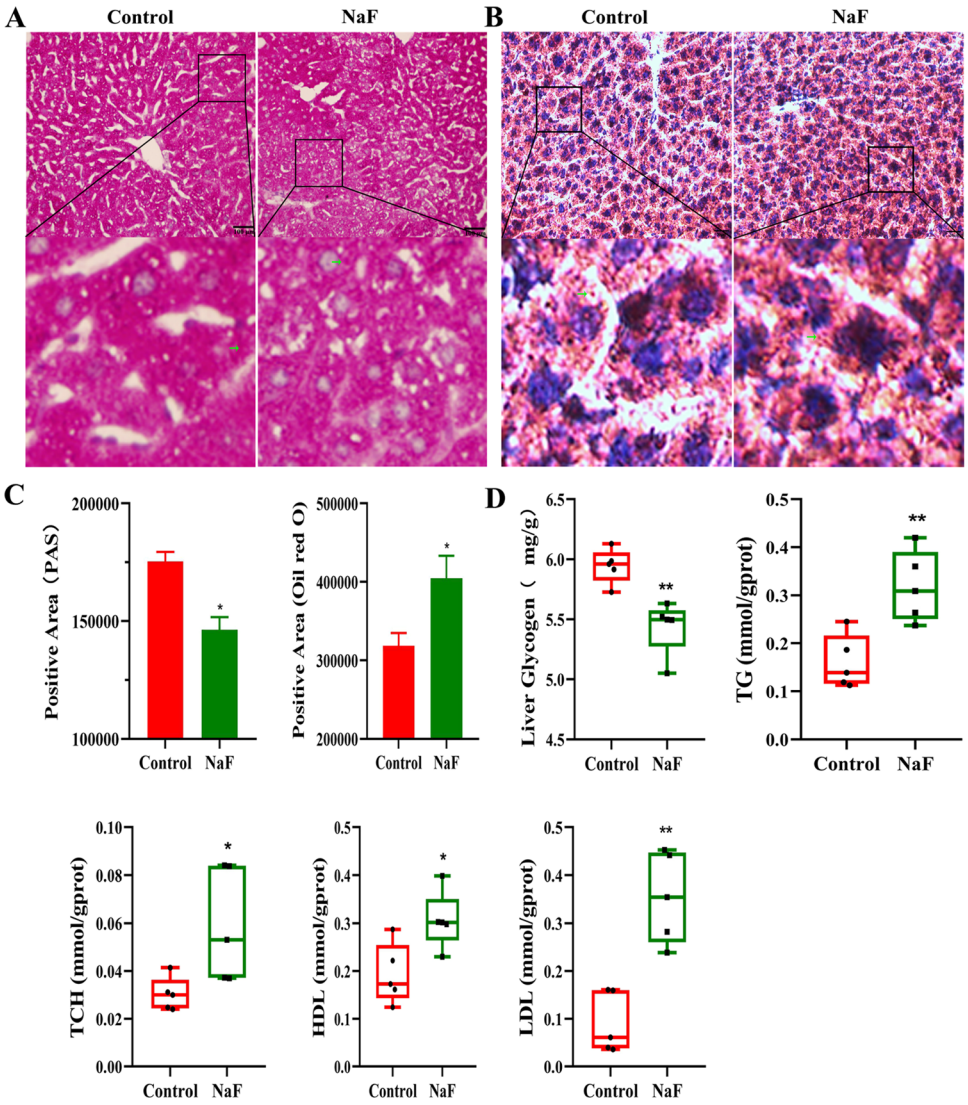

Figure 2. Effects of fluoride on the hepatic glycolipid metabolism. (A) PAS staining, green arrow: positive areas of carbohydrate; (B) Oil Red O staining, green arrow: positive areas of lipids. (C) Statistical results of the positive area of PAS staining and Oil Red O staining. (D) Liver glycogen, TG, TCH, HDL, and LDL levels.

(60 μg), electrophoresis (80 V, 30 min; 100 V, 90 min), membrane transfer (350 mA, 1 h), blocking with nonfat milk (37 °C, 2 h), and primary antibody incubation (4 °C overnight) were performed sequentially. Primary antibody dilution: β-actin (1:5000), IRS2 (1:1000), MYC (1:1000), FASN (1:1000), SCD2 (1:1000), and G6PC (1:1000). Then, the NC membrane was incubated with secondary antibody (37 °C, 2 h, 1:5000) and developed with ECL chemiluminescence (Beyotime, Shanghai, China). Finally, the results were analyzed with the Fluor Chem Q multifunction imaging system (Cell Biosciences, Inc., California). Primary and secondary antibodies were obtained from ABclonal Technology Co., Ltd., Wuhan, China.

Statistical Analysis. The experimental data were presented with mean ± SD. The statistical analysis was performed using the GraphPad Prism 5 software (GraphPad Software Inc., Sandiego). In the statistical analysis, Tukey's test was used to analyze the significance, and $P < 0.05$ was considered statistically significant.

RESULTS

Effects of Fluoride on the Liver Ultrastructure, Microstructure, Fluoride Content, and Function. The HE staining and TEM were used to detect liver microstructure and ultrastructure changes. As shown in Figure 1A, after fluoride exposure, the liver cord arrangement was disordered, and the number of nuclear lysis hepatocytes was increased. Moreover, fluoride elevated the number of lipid droplets in the hepatocytes. In the TEM results, fluoride elevated the number of damaged mitochondria and autophagosomes and reduced the number of mitochondria in the hepatocytes (Figure 1B). The above results suggested that fluoride caused hepatic morphology and ultrastructural injury.

As shown in Figure 1C−E, the liver fluoride content and the levels of ALT and AST were markedly elevated in the fluoride group ($P < 0.05$, $P < 0.01$). These results suggested that fluoride resulted in fluoride accumulation and functional impairment in the liver.

Effects of Fluoride Exposure on Hepatic Glucose and Lipid Metabolism. PAS staining; Oil Red O staining; and the levels of liver glycogen, LDL, HDL, TC, and TG in the liver were used to explore the effects of fluoride on hepatic glycolipid metabolism. The PAS staining results showed that the red color was uniform and widely distributed and lots of red granules (positive areas) were present in the liver of the control group, but the red color became lighter and the positive areas were

https://doi.org/10.1021/acs.jafc.2c03049
J. Agric. Food Chem. 2022, 70, 14284−14295

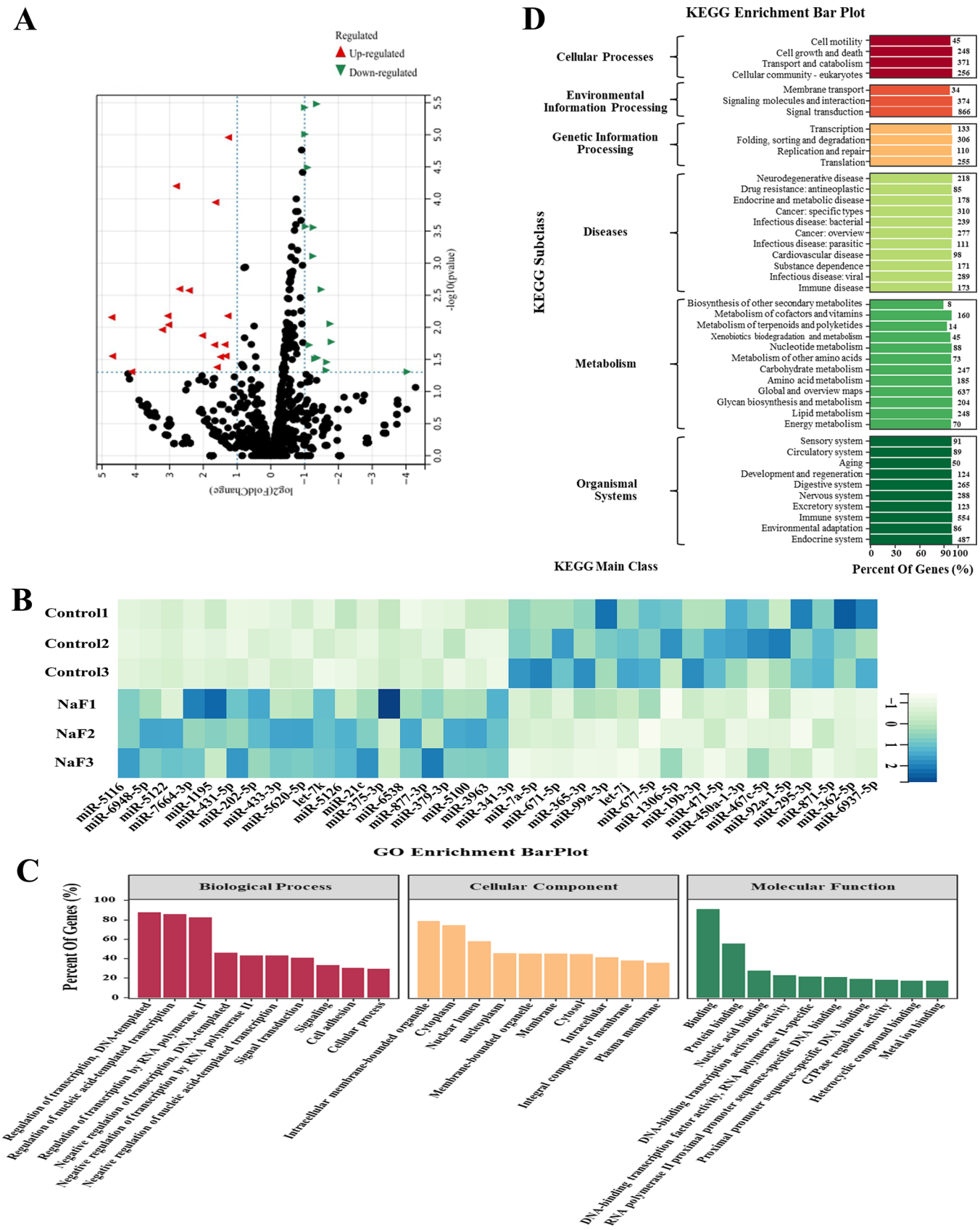

Figure 3. Results of miRNA sequencing. (A) Volcano illustration, $|\log_2 FC| > 1$ and P-value < 0.05; (B) expression heatmap of DE-miRNAs in each sample; (C) GO enrichment histogram; (D) KEGG enrichment histogram.

markedly reduced in the liver of the NaF group (Figure 2A,C, $P < 0.05$). And the liver glycogen assay results showed that fluoride markedly reduced the glycogen content in the liver (Figure 2D, $P < 0.01$). Oil Red O staining results showed that the red was

https://doi.org/10.1021/acs.jafc.2c03049
J. Agric. Food Chem. 2022, 70, 14284−14295

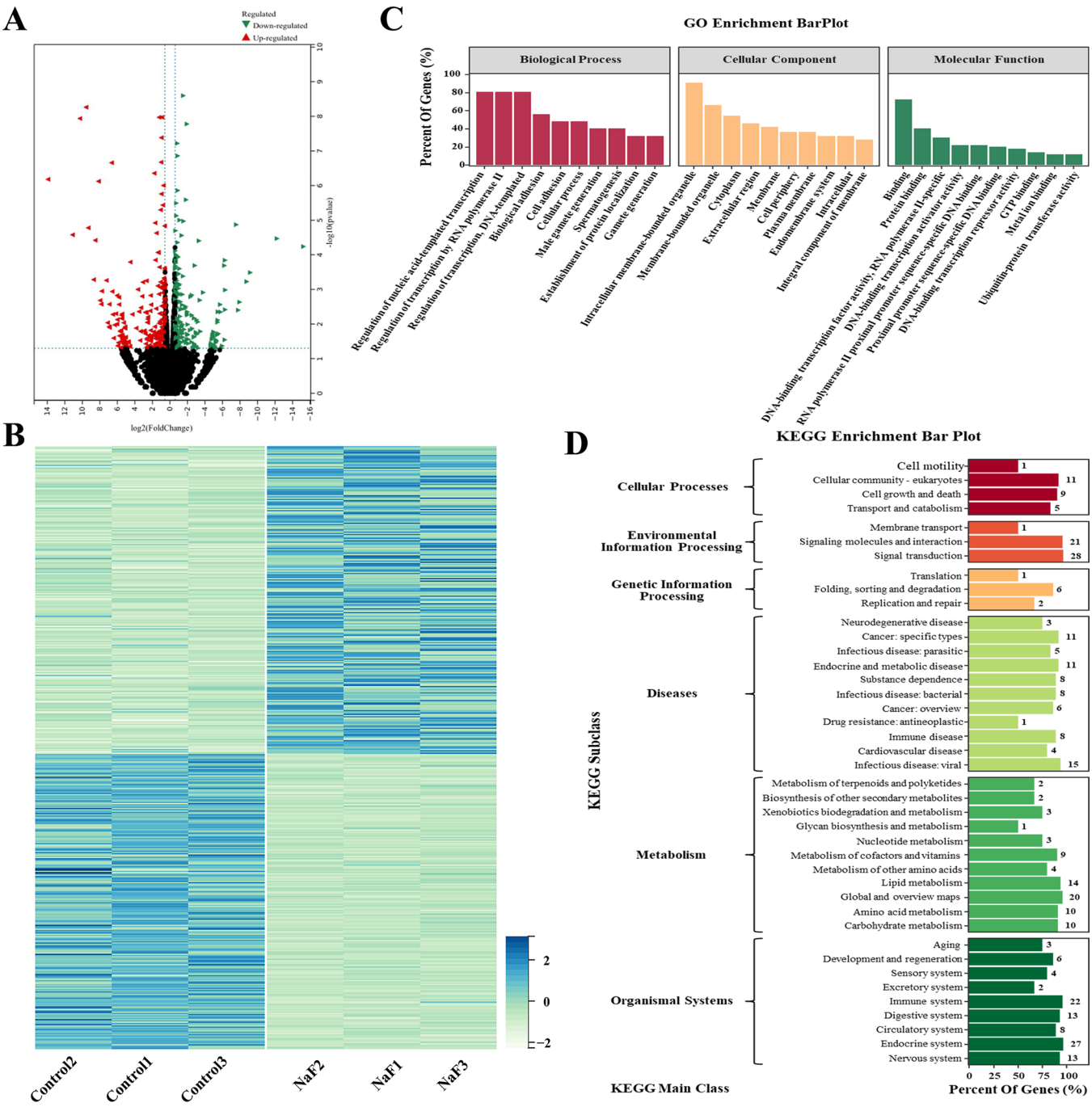

Figure 4. Results of mRNA sequencing. (A) Volcano illustration, $|\log_2 FC| > 0.585$ and P-value < 0.05; (B) expression heatmap of DE-mRNAs in each sample; (C) GO enrichment histogram; (D) KEGG enrichment histogram.

darker, the lipid-positive areas were significantly increased, and the red particles were aggregated in the liver of the NaF group (Figure 2B,C, $P < 0.05$). Besides, the results of the lipid metabolism-related indicators showed that fluoride treatment markedly elevated the contents of TG, TG, LDL, HDL, and TC in the liver (Figure 2D, $P < 0.05$, $P < 0.01$). These results demonstrated that fluoride caused the disorders of liver glycolipid metabolism.

miRNA-Seq and Bioinformatics Analysis of Target mRNAs. The read sequences were compared with the mature miRNA sequence in the known miRNA database (miRBase v21). After analysis, 1023 known miRNAs were compared. The screening conditions were $|\log_2 FC| > 1$ and P-value < 0.05 (Figure 3A). After fluoride exposure, 35 DE-miRNAs were found, of which 17 DE-miRNAs were downregulated and 18 DE-miRNAs were upregulated (Figures 3B and S1).

A total of 14798 target mRNAs were predicted using the TargetScan 7.2, and the bioinformatics analysis of target mRNAs was performed using the OmicStudio tools. As shown in Figure 3C, the GO analysis results showed that the target mRNAs were mainly enriched in regulation of DNA-templated transcription, regulation of nucleic acid-templated transcription, and regulation of transcription by RNA polymerase II (BP); intracellular membrane-bound organelle and cytoplasm (CC); and binding and protein binding (MF). In addition, the KEGG analysis results showed that the KEGG main classes of target mRNAs

https://doi.org/10.1021/acs.jafc.2c03049
J. Agric. Food Chem. 2022, 70, 14284−14295

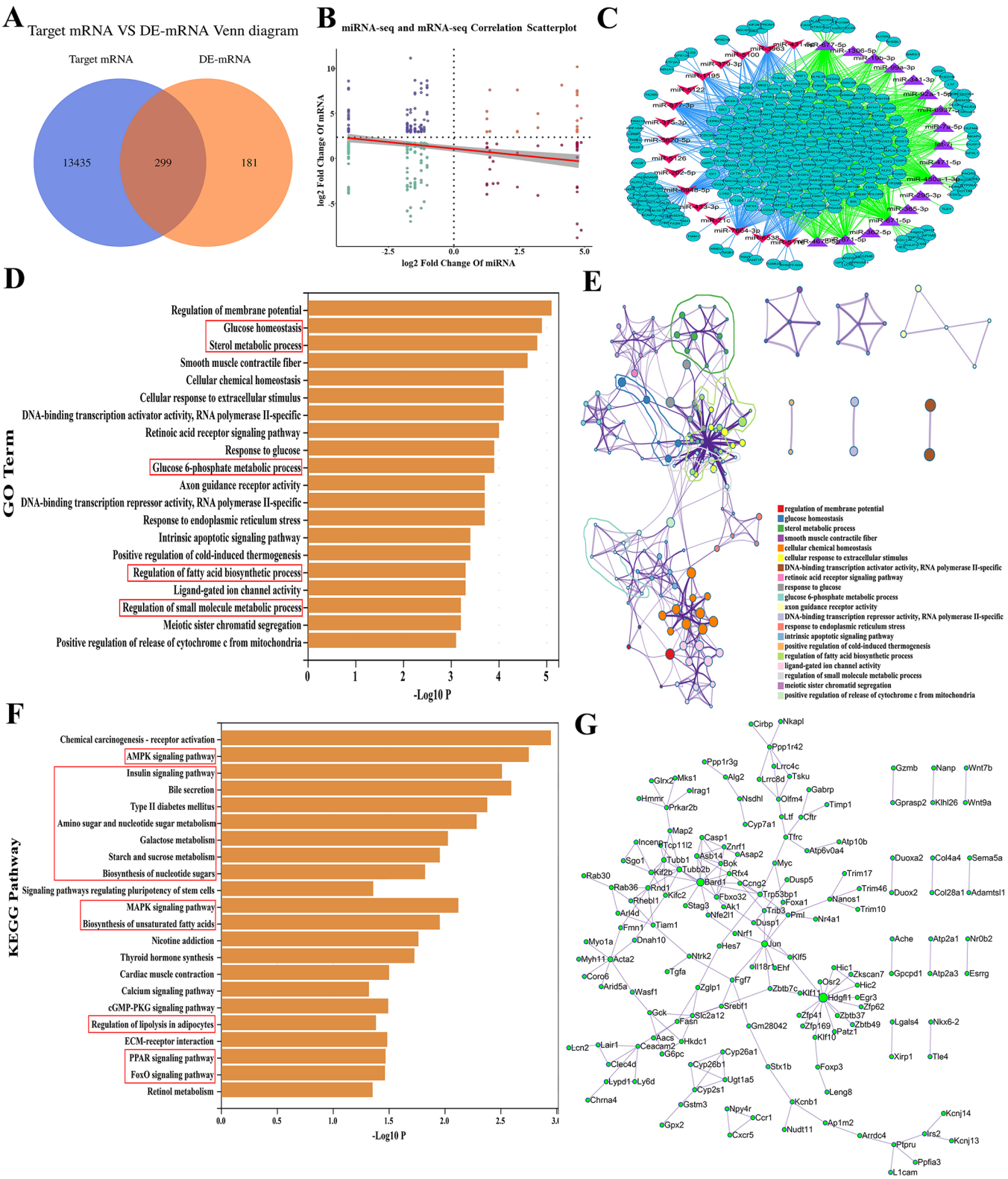

Figure 5. Results of combined analysis of miRNA-seq and mRNA-seq. (A) Venn diagram of target mRNAs vs DE-mRNAs; (B) correlation analysis of DE-miRNAs and DE-mRNAs; (C) network map of DE-miRNAs and DE-mRNAs; (D) GO term enrichment histogram; (E) GO term network map; (F) KEGG enrichment histogram; (G) mRNA network map of DET-mRNAs.

were mainly enriched in diseases, metabolism, and organismal systems. Among them, the metabolism class mainly included lipid metabolism, global and overview maps, glycan biosynthesis and metabolism, amino acid metabolism, carbohydrate metabolism, and metabolism of cofactors and vitamins (Figure 3D).

mRNA-Seq and Bioinformatics Analysis of DE-mRNAs. According to the expression level of mRNAs in the sequencing results, $|\log_2 FC| > 0.585$ and P-value < 0.05 were used as the screening condition, and 480 DE-mRNAs were screened out (Figure 4A). Among them, the expressions of 235 mRNAs were

https://doi.org/10.1021/acs.jafc.2c03049
J. Agric. Food Chem. 2022, 70, 14284−14295

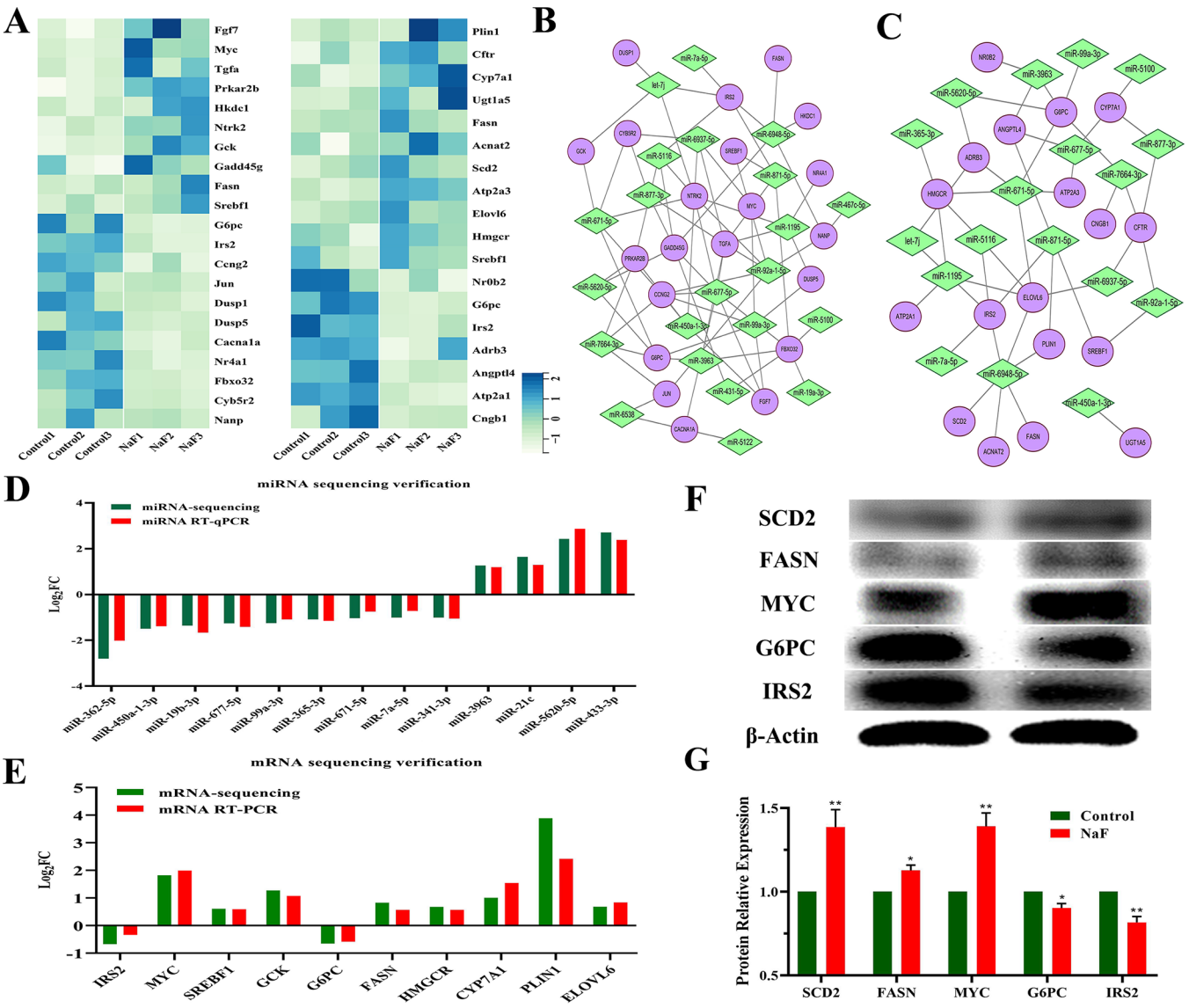

Figure 6. Effects of fluoride on the expression levels of hepatic glycolipid metabolism-related miRNAs, mRNAs, and proteins. (A) Expression heatmap of hepatic glycolipid metabolism-related miRNAs and mRNAs in each sample; (B) glucose metabolism-related miRNA−mRNA network map; (C) lipid metabolism-related miRNA−mRNA network map; (D) RT-PCR verification results of miRNA-seq; (E) RT-PCR verification results of mRNA-seq; (F) protein bands; (G) protein relative expression of key differential genes.

decreased and the expressions of 245 mRNAs were increased (Figure 4B).

The OmicStudio tools were used to perform the bioinformatics analysis of DE-mRNAs. As shown in Figure 4C, the GO analysis results showed that the DE-mRNAs were mainly enriched in regulation of nucleic acid-templated transcription, regulation of transcription by RNA polymerase II, regulation of DNA-templated transcription, and biological adhesion (BP); intracellular membrane-bound organelle, membrane-bound organelle, cytoplasm, extracellular region, and membrane (CC); and binding, protein binding, DNA-binding transcription factor activity, and RNA polymerase II-specific (MF). The KEGG main classes of target mRNAs and DE-mRNAs were similar, and the DE-mRNAs were mainly enriched in carbohydrate metabolism, amino acid metabolism, global and overview maps, lipid metabolism, and metabolism of cofactors and vitamins in the metabolism class (Figure 4D).

Coanalysis of miRNA-Seq and mRNA-Seq. Correlation analysis of mRNA-seq and miRNA-seq was used to detect the correlation trend, and the results showed that the mRNA-seq and miRNA-seq were negatively correlated (Figure 5B). In addition, the target mRNAs of miRNAs were mapped to the mRNA sequence results, and 299 mRNAs were obtained (Figure 5A, Table S1). The 299 differentially expressed target (DET)-mRNAs were regulated by 34 DE-miRNAs. Among them, 17 upregulated miRNAs regulated 250 DET-mRNAs and 17 downregulated miRNAs regulated 85 DET-mRNAs. The miRNA−mRNA network is shown in Figure 5C, and the network of DET-mRNAs is shown in Figure 5G.

The bioinformatics analysis of DET-mRNAs was performed using the Sangerbox 3.0 and Metascape, and the GO and KEGG analyses were used to study miRNA functions. The GO analysis results showed that DET-mRNAs mainly enriched in the regulation of membrane potential, glucose homeostasis, sterol metabolic process, smooth muscle contractile fiber, cellular chemical homeostasis, cellular response to extracellular stimulus, retinoic acid receptor signaling pathway, response to glucose, glucose 6-phosphate metabolic process, axon guidance receptor

https://doi.org/10.1021/acs.jafc.2c03049
J. Agric. Food Chem. 2022, 70, 14284−14295

activity, DNA-binding transcription activator activity, RNA polymerase II-specific, response to endoplasmic reticulum stress, intrinsic apoptotic signaling pathway, positive regulation of cold-induced thermogenesis, regulation of fatty acid biosynthetic process, ligand-gated ion channel activity, regulation of small-molecule metabolic process, meiotic sister chromatid segregation, and positive regulation of release of cytochrome *c* from mitochondria (Figure 5D), and the interaction network of the top 20 GO terms is shown in Figure 5E. Moreover, the KEGG analysis results showed that DET-mRNAs mainly enriched in the chemical carcinogenesis-receptor activation, AMPK signaling pathway, bile secretion, insulin signaling pathway, type II diabetes mellitus, amino sugar and nucleotide sugar metabolism, MAPK signaling pathway, galactose metabolism, starch and sucrose metabolism, biosynthesis of unsaturated fatty acids, biosynthesis of nucleotide sugars, nicotine addiction, thyroid hormone synthesis, cardiac muscle contraction, cGMP-PKG signaling pathway, ECM-receptor interaction, PPAR signaling pathway, FOXO signaling pathway, regulation of lipolysis in adipocytes, signaling pathways regulating pluripotency of stem cells, and retinol metabolism (Figure 5F).

Analysis of the Role of DET-mRNAs in Glycolipid Metabolism. To further reveal the role of miRNAs in hepatic lipid metabolism under fluoride exposure, the glycolipid metabolism-related DET-mRNAs were screened for further miRNA−mRNA network analysis. Among the 22 pathways enriched for DET-mRNAs, 13 pathways were related to glycolipid metabolism (Figure 5F; insulin signaling pathway, AMPK signaling pathway, MAPK signaling pathway, PPAR signaling pathway, FOXO signaling pathway, bile secretion, type II diabetes mellitus, amino sugar and nucleotide sugar metabolism, galactose metabolism, starch and sucrose metabolism, biosynthesis of unsaturated fatty acids, biosynthesis of nucleotide sugars, regulation of lipolysis in adipocytes). A total of 36 DET-mRNAs map to these 13 pathways (Figure 6A). Among them, FASN, G6PC, PRKAR2B, SREBF1, GCK, HKDC1, IRS2, CACNA1A, NANP, CYB5R2, FGF7, NR4A1, JUN, MYC, NTRK2, DUSP1, TGFA, GADD45G, DUSP5, CCNG2, and FBXO32 were related to glucose metabolism, which were regulated by miR-6937−5p, miR-871-5p, miR-92a-1-5p, miR-467c-5p, miR-450a-1-3p, miR-19a-3p, miR-677-5p, miR-99a-3p, let-7j, miR-671-5p, miR-7a-5p, miR-3963, miR-5100, miR-877-3p, miR-6538, miR-5620-5p, miR-431-5p, miR-1195, miR-7664-3p, miR-5122, miR-6948-5p, and miR-5116 (Figure 6B). In addition, CFTR, FASN, G6PC, HMGCR, SCD2, SREBF1, IRS2, CYP7A1, NR0B2, ACNAT2, UGT1A5, ELOVL6, ADRB3, ATP2A1, ATP2A3, CNGB1, PLIN1, ANGPTL4 were related to lipid metabolism, which were regulated by miR-6937-5p, miR-871-5p, miR-92a-1-5p, miR-450a-1-3p, miR-677-5p, miR-99a-3p, let-7j, miR-365-3p, miR-671-5p, miR-7a-5p, miR-3963, miR-5100, miR-877-3p, miR-5620-5p, miR-1195, miR-7664-3p, miR-6948-5p, and miR-5116 (Figure 6C). The expression levels of glycolipid metabolism-related DET-mRNAs in the different groups are shown in Figure 6A, and the miRNA−mRNA interaction networks of glycolipid metabolism are shown in Figure 6B,C.

Effects of Fluoride on the Expression Levels of Hepatic Glycolipid Metabolism-Related miRNAs, mRNAs, and Proteins and Verification of miRNA-Seq and mRNA-Seq Results. RT-PCR was used to detect the expressions of glucose metabolism-related 13 DE-miRNAs and 10 DE-mRNAs and verify the results of miRNA-seq and mRNA-seq. As shown in Figure 6D, the expression levels of miR-362-5p, miR-450a-1-3p, miR-19b-3p, miR-677-5p, miR-99a-3p, miR-365-3p, miR-671-5p, miR-7a-5p, and miR-341-3p were decreased, while the expression levels of miR-3963, miR-21c, miR-5620-5p, and miR-433-3p were increased in the fluoride group. In addition, the fluoride treatment increased the mRNA expression of MYC, SREBF1, GCK, FASN, HMGCR, CYP7A1, PLIN1, and ELOVL6 and reduced the mRNA expression of IRS2 and G6PC (Figure 6E). Moreover, the protein expressions of key differential genes were detected using the western blotting (IRS2, MYC, FASN, SCD2, and G6PC) in the glycolipid metabolism-related pathways (Insulin pathway, MAPK pathway, AMPK pathway, PPAR pathway, and FOXO pathway). The results showed that fluoride elevated the protein expression of MYC, FASN, and SCD2 but reduced the protein expression of IRS2 and G6PC (Figure 6F,G). These results indicated that fluoride disturbed the liver glycolipid metabolism. Besides, the change trends of miRNAs, mRNAs, and proteins were consistent with the results of miRNA-seq and mRNA-seq, which suggested that the sequencing results were reliable.

■ DISCUSSION

Excessive fluoride exposure can result in the damage of multiple organs.[4] As an essential digestive and detoxification organ, the liver is a significant target organ for fluoride.[5,18] Our previous works have found that long-term chronic fluoride exposure results in massive fluoride accumulation in the liver, which destroys the liver histomorphology and function.[6,19] Similar to our previous research, in this study, fluoride induced the damage of morphology and ultrastructure and elevated the levels of AST and ALT in the liver, which suggested that fluoride gave rise to the morphological and functional injury of the liver.

Glucoses and lipids are the primary sources of energy for sustaining life activities,[20] and the homeostasis of their regulatory networks is also a critical inducing factor in the various metabolic diseases. As the most important metabolic organ, the liver plays a significant role in regulating glycolipid metabolism homeostasis in the body.[9] Literatures have reported that fluoride could affect the biological processes of gluconeogenesis, glycolysis, and lipid peroxidation, resulting in decreased carbohydrates and increased lipids in the liver, which disrupts the homeostasis of glycolipid metabolism in the body.[21,22] These findings were confirmed in this study; fluoride caused the reduction of glycogen content and the increase of the number of lipid droplets and the content of TG, TC, HDL, and LDL in the liver, which suggested that fluoride resulted in the disturbances of hepatic glycolipid metabolism.

Recent research studies have proved that miRNAs play a significant regulatory role in the liver glycolipid metabolism,[23] but the mechanism of miRNAs in fluoride-induced hepatic glycolipid metabolism disorders is still unclear. Therefore, this study used the miRNA-seq and mRNA-seq to screen the key miRNAs and mRNAs and revealed the regulatory mechanism in fluoride-induced liver glycolipid metabolism disorders. In this study, 35 DE-miRNAs and 480 DE-mRNAs were screened out, and the target mRNAs and DE-mRNAs were mainly enriched in the diseases, organismal system categories, and metabolism in the KEGG. In the disease categories, it is mainly enriched in cancer, endocrine and metabolic disease, immune disease, cardiovascular disease, and infectious disease. In the metabolism categories, it is mainly enriched in the global and overview maps, lipid metabolism, carbohydrate metabolism, metabolism of cofactors and vitamins, and amino acid metabolism. In the

https://doi.org/10.1021/acs.jafc.2c03049
J. Agric. Food Chem. 2022, 70, 14284−14295

organismal system categories, it is mainly enriched in the immune system, endocrine system, nervous system, digestive system, circulatory system, and development and regeneration system. According to these enrichment results, we found that fluoride significantly affected the liver's metabolic and immune biological processes, which has been demonstrated in the previous research. In the study of toads' fluoride exposure, Wang et al. found that fluoride caused changes in the expression levels of fatty acid synthesis and fatty acid oxidation key genes, resulting in disorders of hepatic lipid metabolism.[7] Wang et al. found that fluoride altered the activity of immune-related enzymes and the expression levels of immune-related genes, which further damaged the zebrafish liver.[24] The possible mechanism by which fluoride affects liver metabolism and immunity is that the hepatic fluoride accumulation results in the increase of free radicals in hepatocytes and the damage of mitochondrial and endoplasmic reticulum, which in turn causes fatty acid oxidation disorders, increased lipid synthesis substrates and synthases, and decreased lipolysis. At the same time, some substances released by damaged hepatocytes combine with other substances to form self-antigens and trigger autoimmune responses, which eventually lead to hepatocyte immunopathological damage.[12,25]

To further reveal the mechanism of miRNAs in fluoride-induced hepatic glucose and lipid metabolism disorders, miRNA-seq and mRNA-seq results were conjointly analyzed. After analysis, 299 DET-mRNAs were found. Among the 22 GO terms of GO enrichment, seven GO terms were related to glycolipid metabolism (glucose homeostasis, sterol metabolic process, retinoic acid receptor signaling pathway, response to glucose, glucose 6-phosphate metabolic process, regulation of fatty acid biosynthetic process, regulation of small-molecule metabolic process). In addition, among the 22 pathways of KEGG enrichment, 13 pathways were related to glycolipid metabolism. Among these pathways, insulin signaling pathway, AMPK signaling pathway, MAPK signaling pathway, PPAR signaling pathway, and FOXO signaling pathway are intermediate conduction pathways, and bile secretion, type II diabetes mellitus, amino sugar and nucleotide sugar metabolism, galactose metabolism, starch and sucrose metabolism, biosynthesis of unsaturated fatty acids, biosynthesis of nucleotide sugars, regulation of lipolysis in adipocytes are metabolic process pathways. The regulatory relationships between them are as follows: AMPK is very sensitive to energy changes in the body, and it can increase the β-oxidation of fatty acids and the uptake and utilization of glucose by regulating the biosynthesis of glucose, fatty acids, and cholesterol, thereby stabilizing the intracellular ATP content.[26] As an essential signal transduction pathway, the MAPK pathway is well correlated with insulin resistance, glucose synthesis and transport, and fat synthesis.[8,27] The PPAR pathway can regulate the expression of mitochondrial fatty acid catalytic enzymes, which can regulate the transport of fatty acids to mitochondria by inducing the expression of liver-specific carnitine palmitoyl transportase, stimulate the β-oxidation process, and reduce the synthesis of fatty acids and triacylglycerols.[28] The FOXO pathway can not only regulate the activities of G6pase and PEPCK, gluconeogenesis rate-limiting enzymes, in the gluconeogenesis through the insulin signaling pathway, but also regulate the activities of various enzymes in the synthesis of fatty acids and TG through SREBP-1C, a core gene of adipogenesis.[29] After analyzing the above pathways, we can infer that the hepatic fluoride accumulation activates the insulin pathway, which is transduced by the AMPK and MAPK pathways to change the activation state of the PPAR pathway and the FOXO pathway, and ultimately affects the bile secretion, the metabolic processes of glucose, amino sugars, nucleotide sugars, galactose, starch and sucrose, the decomposition of lipids, and the synthesis of unsaturated fatty acids in the liver.

In this study, fluoride-induced hepatic glucose and lipid metabolism disorders were mainly regulated by 23 miRNAs (miR-6937-5p, miR-871-5p, miR-92a-1-5p, miR-467c-5p, miR-450a-1-3p, miR-19a-3p, miR-677-5p, miR-99a-3p, let-7j, miR-671-5p, miR-7a-5p, miR-3963, miR-5100, miR-877-3p, miR-6538, miR-5620-5p, miR-431-5p, miR-1195, miR-7664-3p, miR-5122, miR-6948-5p, miR-5116, miR-365-3p). These miRNAs have been demonstrated to play critical roles in the glycolipid metabolism. For example, miR-19a-3p is associated with the process of cerebral ischemic injury by adjusting the processes of glucose glycolysis, glucose uptake, and lactate production.[30] Ammonia could reduce ATPase activity through miR-99a-3p, which affected energy metabolism in the chicken bursa.[31] Elevated expression of miR-431-5p could inhibit glycolysis in the hepatoma cells,[32] and miR-431-5p is closely related to the adipogenic process of bone marrow mesenchymal stem cells.[33] Nonetheless, the roles of these miRNAs in fluoride-induced disturbances of hepatic glucose and lipid metabolism need to be further explored.

To verify the reliability of our results, the expression levels of glycolipid metabolism-related 13 miRNAs, 10 mRNAs, and 5 proteins were further detected in this study. Glycolipid metabolism-related genes were IRS2, G6PC, MYC, SREBF1, GCK, FASN, HMGCR, CYP7A1, PLIN1, ELOVL6, and SCD2. IRS2, an important gene in the insulin signaling pathway, is closely related to the process of insulin resistance.[34] G6PC is a rate-limiting enzyme in the gluconeogenesis and glycogenolysis, and the changes of its activity and expression directly affect the output of endogenous sugars.[35] MYC, SREBP1, and FASN are important transcription factors that regulate glycolysis, fatty acid synthesis, and cholesterol synthesis, respectively.[10,36] GCK is the core protein in glucose metabolism and a key kinase involved in regulating intracellular free glucose levels. HMGC and CYP7A1 are key enzymes in cholesterol synthesis. PLIN1 not only regulates the process of lipolysis but also promotes the formation of lipid droplets.[37] ELOVL6 is involved in fatty acid elongation and acyl-CoA biosynthesis.[38] In this study, fluoride reduced the expression of IRS2 and G6PC while elevated the expression of MYC, SREBF1, GCK, FASN, HMGCR, CYP7A1, PLIN1, ELOVL6, and SCD2. These results suggested that fluoride induced the disturbance of hepatic glycolipid metabolism, which further verified the results of morphological and glycolipid metabolism index detection. Besides, the expressions of miR-362-5p, miR-450a-1-3p, miR-19b-3p, miR-677-5p, miR-99a-3p, miR-365-3p, miR-671-5p, miR-7a-5p, and miR-341-3p were decreased, but the expressions of miR-3963, miR-21c, miR-5620-5p, and miR-433-3p were increased after fluoride exposure. These miRNAs have been confirmed to be closely related the process of glycolipid metabolism,[31] for example, miR-19b-3p regulated muscle glucose metabolism.[39] miR-362-5p promoted the proliferation of trophoblast cells by regulating glucose metabolism.[40] Inhibiting the expression of miR-7a-5p promoted LPS-induced myocardial damage.[41] Hence, it can be seen that the above miRNAs play a significant role in fluoride-induced hepatic glycolipid metabolism disorders, which will provide a future research direction for fluoride-induced disturbance of hepatic glycolipid metabolism. Moreover, the mRNA and mRNA RT-PCR results were similar to the

https://doi.org/10.1021/acs.jafc.2c03049
J. Agric. Food Chem. 2022, 70, 14284−14295

sequencing results, which indicated that the sequencing results were reliable.

In summary, fluoride exposure resulted in increased fluoride content, impaired structure and function, and the disturbance of glycolipid metabolism in the liver. Meanwhile, the sequencing results showed that fluoride exposure altered the expression levels of 35 miRNAs and 480 mRNAs in the liver. Further coanalysis obtained 299 DET-mRNAs, and five of the top 20 GO terms and 13 of the top 22 KEGG were related to glycolipid metabolism, regulated by 23 DE-miRNAs. In addition, the expression levels of the glycolipid metabolism key miRNAs and mRNAs were verified, and the reliability of the sequencing results was confirmed. These results indicated that miRNAs are involved in fluoride-induced hepatic glycolipid metabolism disorders by regulating the insulin pathway, PPAR pathway, and the FOXO pathway and in turn affecting the biological process of the bile secretion, the metabolic processes of glucose, amino sugars, nucleotide sugars, galactose, starch and sucrose, the synthesis of unsaturated fatty acids, and the decomposition of lipids in the liver. The screened miRNAs and mRNAs may serve as biomarkers and therapeutic targets of fluorotoxic liver injury, which will be further explored in future research.

■ ASSOCIATED CONTENT

Supporting Information

The Supporting Information is available free of charge at https://pubs.acs.org/doi/10.1021/acs.jafc.2c03049.

miRNAs and the counts for their target mRNAs and $\log_2$FC histogram and $-\log_{10}P$-value histogram of differentially expressed miRNAs (PDF)

■ AUTHOR INFORMATION

Corresponding Author

Jundong Wang − *College of Veterinary Medicine, Shanxi Agricultural University, Taigu, Shanxi 030801, China;* orcid.org/0000-0002-8767-3659; Email: wangjd53@outlook.com

Authors

Yangfei Zhao − *College of Veterinary Medicine, Shanxi Agricultural University, Taigu, Shanxi 030801, China*

Yanghuan Yu − *College of Veterinary Medicine, Shanxi Agricultural University, Taigu, Shanxi 030801, China*

Mohammad Mehdi Ommati − *College of Life Sciences, Shanxi Agricultural University, Taigu, Shanxi 030801, China; Pharmaceutical Sciences Research Center, Shiraz University of Medical Sciences, Shiraz 71348-14336, Iran;* orcid.org/0000-0003-0514-2414

Jipeng Xu − *College of Veterinary Medicine, Shanxi Agricultural University, Taigu, Shanxi 030801, China*

Jinming Wang − *College of Veterinary Medicine, Shanxi Agricultural University, Taigu, Shanxi 030801, China*

Jianhai Zhang − *College of Veterinary Medicine, Shanxi Agricultural University, Taigu, Shanxi 030801, China;* orcid.org/0000-0001-6005-8376

Zilong Sun − *College of Veterinary Medicine, Shanxi Agricultural University, Taigu, Shanxi 030801, China;* orcid.org/0000-0003-4907-7271

Ruiyan Niu − *College of Veterinary Medicine, Shanxi Agricultural University, Taigu, Shanxi 030801, China*

Complete contact information is available at: https://pubs.acs.org/10.1021/acs.jafc.2c03049

Author Contributions

Y.Z.: Conceptualization, formal analysis, investigation, writing—original draft. Y.Y.: Validation, methodology. M.M.O.: Validation, writing—review & editing. J.X.: Formal analysis. Jinming Wang: Writing—review & editing, supervision. J.Z.: Supervision. Z.S.: Supervision. R.N.: Writing—review & editing. Jundong Wang: Project administration, supervision, funding acquisition.

Funding

This research was supported by the National Natural Science Foundation of China (31672623, 31372497), Scientific Research Project of Shanxi Province Outstanding Doctoral Work Award Foundation (SXYBKY2019047), Fundamental Research Program of Shanxi Province (20210302124063), and Innovation Projects of College of Veterinary Medicine, Shanxi Agricultural University (DY-Q014).

Notes

The authors declare no competing financial interest.

■ ABBREVIATIONS AND NOMENCLATURE

ALT, glutamic pyruvic transaminase; AST, glutamic oxaloacetic transaminase; DE, differentially expressed; DET, differentially expressed target; GO, Gene Ontology; HDL, high-density lipoprotein; LDL, low-density lipoprotein; miRNA, microRNA; seq, sequencing; NaF, sodium fluoride; TC, total cholesterol; TG, triglyceride

■ REFERENCES

(1) Zhou, G.; Hu, Y.; Wang, A.; Guo, M.; Du, Y.; Gong, Y.; Ding, L.; Feng, Z.; Hou, X.; Xu, K.; Yu, F.; Li, Z.; Ba, Y. Fluoride Stimulates Anxiety- and Depression-like Behaviors Associated with SIK2-CRTC1 Signaling Dysfunction. *J. Agric. Food Chem.* **2021**, *69*, 13618−13627.

(2) Wang, J.; Zhan, C.; Chen, Y.; Li, J.; Hong, J.; Wang, W.; Cai, J. A study of damage to hard tissue of goats due to industrial fluoride pollution. *Fluoride* **1992**, *25*, 123−130.

(3) Riddell, J. K.; Malin, A.; Flora, D.; McCague, H.; Till, C. Association of water fluoride and urinary fluoride concentrations with attention deficit hyperactivity disorder in Canadian youth. *Environ. Int.* **2019**, *133*, No. 105190.

(4) Wang, J.; Xu, H.; Cheng, X.; Yang, J.; Yan, Z.; Ma, H.; Zhao, Y.; Ommati, M. M.; Manthari, R. K.; Wang, J. Calcium relieves fluoride-induced bone damage through the PI3K/AKT pathway. *Food Funct.* **2020**, *11*, 1155−1164.

(5) Malin, A. J.; Lesseur, C.; Busgang, S.; Curtin, P.; Wright, R.; Sanders, A. Fluoride exposure and kidney and liver function among adolescents in the United States: NHANES, 2013-2016. *Environ. Int.* **2019**, *132*, No. 105012.

(6) Zhao, Y.; Wang, J.; Zhang, J.; Sun, Z.; Niu, R.; Manthari, R.; Ommati, M.; Wang, S.; Wang, J. Fluoride exposure induces mitochondrial damage and mitophagy via activation of the IL-17A pathway in hepatocytes. *Sci. Total Environ.* **2022**, *804*, No. 150184.

(7) Wang, X.; Zheng, R.; Yao, Q.; Liang, Z.; Wu, M.; Wang, H. Effects of fluoride on the histology, lipid metabolism, and bile acid secretion in liver of Bufo gargarizans larvae. *Environ. Pollut.* **2019**, *254*, No. 113052.

(8) Cui, X.; Qian, D.; Jiang, S.; Shang, E.; Zhu, Z.; Duan, J. Scutellariae Radix and Coptidis Rhizoma Improve Glucose and Lipid Metabolism in T2DM Rats via Regulation of the Metabolic Profiling and MAPK/PI3K/Akt Signaling Pathway. *Int. J. Mol. Sci.* **2018**, *19*, 3634.

(9) Lewis, G. F.; Carpentier, A.; Pereira, S.; Hahn, M.; Giacca, A. Direct and indirect control of hepatic glucose production by insulin. *Cell Metab.* **2021**, *33*, 709−720.

(10) Chen, J.; Ding, C.; Chen, Y.; Hu, W.; Yu, C.; Peng, C.; Feng, X.; Cheng, Q.; Wu, W.; Lu, Y.; Xie, H.; Zhou, L.; Wu, J.; Zheng, S. ACSL4 reprograms fatty acid metabolism in hepatocellular carcinoma via c-Myc/SREBP1 pathway. *Cancer Lett.* **2021**, *502*, 154−165.

(11) Liu, J.; Dong, C.; Zhai, Z.; Tang, L.; Wang, L. Glyphosate-induced lipid metabolism disorder contributes to hepatotoxicity in juvenile common carp. *Environ. Pollut.* **2021**, *269*, No. 116186.
(12) Trevizol, J. S.; Buzalaf, N.; Dionizio, A.; Delgado, A.; Cestari, T.; Bosqueiro, J.; Magalhães, A.; Buzalaf, M. Effects of low-level fluoride exposure on glucose homeostasis in female NOD mice. *Chemosphere* **2020**, *254*, No. 126602.
(13) Sharma, P.; Verma, P.; Sood, S.; Singh, M.; Verma, D. Impact of Chronic Sodium Fluoride Toxicity on Antioxidant Capacity, Biochemical Parameters, and Histomorphology in Cardiac, Hepatic, and Renal Tissues of Wistar Rats. *Biol. Trace Elem. Res.* **2022**, DOI: 10.1007/s12011-022-03113-w.
(14) Tan, B. W.; Sim, W.; Cheong, J.; Kuan, W.; Tran, T.; Lim, H. MicroRNAs in chronic airway diseases: Clinical correlation and translational applications. *Pharmacol. Res.* **2020**, *160*, No. 105045.
(15) Chen, L.; Heikkinen, L.; Wang, C.; Yang, Y.; Sun, H.; Wong, G. Trends in the development of miRNA bioinformatics tools. *Briefings Bioinf.* **2019**, *20*, 1836−1852.
(16) Price, N. L.; Zhang, X.; Fernández-Tussy, P.; Singh, A.; Burnap, S.; Rotllan, N.; Goedeke, L.; Sun, J.; Canfrán-Duque, A.; Aryal, B.; Mayr, M.; Suárez, Y.; Fernández-Hernando, C. Loss of hepatic miR-33 improves metabolic homeostasis and liver function without altering body weight or atherosclerosis. *Proc. Natl. Acad. Sci. U.S.A.* **2021**, *118*, No. e2006478118.
(17) Seok, S.; Sun, H.; Kim, Y.; Kemper, B.; Kemper, J. miR-802Defective FXR-SHP Regulation in Obesity Aberrantly Increases Expression, Promoting Insulin Resistance and Fatty Liver. *Diabetes* **2021**, *70*, 733−744.
(18) Dec, K.; Łukomska, A.; Baranowska-Bosiacka, I.; Pilutin, A.; Maciejewska, D.; Skonieczna-Żydecka, K.; Derkacz, R.; Goschorska, M.; Wąsik, A.; Rębacz-Maron, E.; Gutowska, I. Pre-and postnatal exposition to fluorides induce changes in rats liver morphology by impairment of antioxidant defense mechanisms and COX induction. *Chemosphere* **2018**, *211*, 112−119.
(19) Zhao, Y.; Li, Y.; Wang, J.; Manthari, R.; Wang, J. Fluoride induces apoptosis and autophagy through the IL-17 signaling pathway in mice hepatocytes. *Arch. Toxicol.* **2018**, *92*, 3277−3289.
(20) Dimitriadis, G. D.; Maratou, E.; Kountouri, A.; Board, M.; Lambadiari, V. Regulation of Postabsorptive and Postprandial Glucose Metabolism by Insulin-Dependent and Insulin-Independent Mechanisms: An Integrative Approach. *Nutrients* **2021**, *13*, 159.
(21) Dionizio, A.; Pereira, H.; Araujo, T.; Sabino-Arias, I.; Fernandes, M.; Oliveira, K.; Raymundo, F.; Cestari, T.; Nogueira, F.; Carvalho, R.; Buzalaf, M. Effect of Duration of Exposure to Fluoride and Type of Diet on Lipid Parameters and De Novo Lipogenesis. *Biol. Trace Elem. Res.* **2019**, *190*, 157−171.
(22) Li, L.; Lin, L.; Deng, J.; Lin, X.; Li, Y.; Xia, B. The therapeutic effects of Prunella vulgaris against fluoride-induced oxidative damage by using the metabolomics method. *Environ. Toxicol.* **2021**, *36*, 1802−1816.
(23) Qian, G.; Morral, N. Role of non-coding RNAs on liver metabolism and NAFLD pathogenesis. *Hum. Mol. Genet.* **2022**, *10*, No. ddac088.
(24) Wang, G.; Wang, T.; Zhang, X.; Chen, J.; Feng, C.; Yun, S.; Cheng, Y.; Cheng, F.; Cao, J. Sex-specific effects of fluoride and lead exposures on histology, antioxidant physiology, and immune system in the liver of zebrafish (*Danio rerio*). *Ecotoxicology* **2022**, *31*, 396−414.
(25) Cao, J.; Feng, C.; Xie, L.; Li, L.; Chen, J.; Yun, S.; Guo, W.; Wang, T.; Wu, Y.; Meng, R.; Wang, G.; He, X.; Luo, Y. Sesamin attenuates histological alterations, oxidative stress and expressions of immune-related genes in liver of zebrafish (*Danio rerio*) exposed to fluoride. *Fish Shellfish Immunol.* **2020**, *106*, 715−723.
(26) Sun, W.-X.; Lou, K.; Chen, L.; Liu, S.; Pang, S. Lipocalin-2: a role in hepatic gluconeogenesis via AMP-activated protein kinase (AMPK). *J. Endocrinol. Invest.* **2021**, *44*, 1753−1765.
(27) Yu, L.; Yang, X.; Ma, B.; Ying, H.; Shang, X.; He, B.; Zhang, Q. Abnormal arachidonic acid metabolic network may reduce sperm motility via P38 MAPK. *Open Biol.* **2019**, *9*, No. 180091.
(28) Francque, S.; Szabo, G.; Abdelmalek, M.; Byrne, C.; Cusi, K.; Dufour, J.; Roden, M.; Sacks, F.; Tacke, F. Nonalcoholic steatohepatitis: the role of peroxisome proliferator-activated receptors. *Nat. Rev. Gastroenterol. Hepatol.* **2021**, *18*, 24−39.
(29) Bhardwaj, G.; Penniman, C.; Jena, J.; Suarez Beltran, P.; Foster, C.; Poro, K.; Junck, T.; Hinton, A.; Souvenir, R.; Fuqua, J.; Morales, P.; Bravo-Sagua, R.; Sivitz, W.; Lira, V.; Abel, E.; O'Neill, B. Insulin and IGF-1 receptors regulate complex I-dependent mitochondrial bioenergetics and supercomplexes via FoxOs in muscle. *J. Clin. Invest.* **2021**, *131*, No. e146415.
(30) Ge, X.-L.; Wang, J.; Liu, X.; Zhang, J.; Liu, C.; Guo, L. Inhibition of miR-19a protects neurons against ischemic stroke through modulating glucose metabolism and neuronal apoptosis. *Cell. Mol. Biol. Lett.* **2019**, *24*, 37.
(31) Ali Shah, S. W.; Zhang, S.; Ishfaq, M.; Tang, Y.; Teng, X. PTEN/AKT/mTOR pathway involvement in autophagy, mediated by miR-99a-3p and energy metabolism in ammonia-exposed chicken bursal lymphocytes. *Poult. Sci.* **2021**, *100*, 553−564.
(32) Lu, H.; Gao, L.; Lv, J. Circ_0078710 promotes the development of liver cancer by upregulating TXNDC5 via miR-431-5p. *Ann. Hepatol.* **2022**, *27*, No. 100551.
(33) Zhi, F.; Ding, Y.; Wang, R.; Yang, Y.; Luo, K.; Hua, F. Exosomal hsa_circ_0006859 is a potential biomarker for postmenopausal osteoporosis and enhances adipogenic versus osteogenic differentiation in human bone marrow mesenchymal stem cells by sponging miR-431-5p. *Stem Cell Res. Ther.* **2021**, *12*, 157.
(34) Yue, X.; Han, T.; Hao, W.; Wang, M.; Fu, Y. SHP2 knockdown ameliorates liver insulin resistance by activating IRS-2 phosphorylation through the AKT and ERK1/2 signaling pathways. *FEBS Open Bio* **2020**, *10*, 2578−2587.
(35) Youn, D. Y.; Xiaoli, A.; Zong, H.; Okada, J.; Liu, L.; Pessin, J.; Pessin, J.; Yang, F. The Mediator complex kinase module is necessary for fructose regulation of liver glycogen levels through induction of glucose-6-phosphatase catalytic subunit (G6pc). *Mol. Metab.* **2021**, *48*, No. 101227.
(36) Lafita-Navarro, M. C.; Perez-Castro, L.; Zacharias, L.; Barnes, S.; DeBerardinis, R.; Conacci-Sorrell, M. The transcription factors aryl hydrocarbon receptor and MYC cooperate in the regulation of cellular metabolism. *J. Biol. Chem.* **2020**, *295*, 12398−12407.
(37) Zusi, C.; Rinaldi, E.; Bonetti, S.; Boselli, M.; Trabetti, E.; Malerba, G.; Bonora, E.; Bonadonna, R.; Trombetta, M. Haplotypes of the genes (GCK and G6PC2) underlying the glucose/glucose-6-phosphate cycle are associated with pancreatic beta cell glucose sensitivity in patients with newly diagnosed type 2 diabetes from the VNDS study (VNDS 11). *J. Endocrinol. Invest.* **2021**, *44*, 2567−2574.
(38) Junjvlieke, Z.; Khan, R.; Mei, C.; Cheng, G.; Wang, S.; Raza, S.; Hong, J.; Wang, X.; Yang, W.; Zan, L. Effect of ELOVL6 on the lipid metabolism of bovine adipocytes. *Genomics* **2020**, *112*, 2282−2290.
(39) Massart, J.; Sjögren, R.; Egan, B.; Garde, C.; Lindgren, M.; Gu, W.; Ferreira, D.; Katayama, M.; Ruas, J.; Barrès, R.; O'Gorman, D.; Zierath, J.; Krook, A. Endurance exercise training-responsive miR-19b-3p improves skeletal muscle glucose metabolism. *Nat. Commun.* **2021**, *12*, No. 5948.
(40) Zhang, C.; Zhao, D. MicroRNA-362-5p promotes the proliferation and inhibits apoptosis of trophoblast cells via targeting glutathione-disulfide reductase. *Bioengineered* **2021**, *12*, 2410−2419.
(41) Liang, D.; Jin, Y.; Lin, M.; Xia, X.; Chen, X.; Huang, A. Down-regulation of Xist and Mir-7a-5p improves LPS-induced myocardial injury. *Int. J. Med. Sci.* **2020**, *17*, 2570−2577.